

Gas pressure sintering of β -silicon nitride

M. MITOMO

National Institute for Research in Inorganic Materials, 1-1 Namiki, Tsukuba-shi, Ibaraki 305, Japan

S. UENOSONO

High-Technology Research Institute, Kawasaki Steel Corp., 1 Kawasaki-cho, Chiba 260, Japan

The sintering behaviour of β - Si_3N_4 powder was investigated in 980 kPa (10 atm) nitrogen at 1800–2000 °C. It is shown that β - Si_3N_4 has a higher sinterability than the finer α - Si_3N_4 . The solution of small grains and reprecipitation on large grains occurred during sintering at >1600 °C. The rate-determining step in the liquid-phase sintering is believed to be the diffusion of material through the liquid phase at grain boundaries. There was no abnormal grain growth during gas pressure sintering of β - Si_3N_4 . The microstructures of gas pressure sintered materials from β - Si_3N_4 were more uniform than those from α - Si_3N_4 . The densification mechanism of β - Si_3N_4 is discussed in relation to that of α - Si_3N_4 .

1. Introduction

One of the most important properties of silicon nitride ceramics for their application as engineering materials is the fracture toughness. It has been reported that starting powders with high α -content developed rod-like grains during hot-pressing, and this resulted in high fracture toughness [1, 2]. The same results were obtained for hot-isostatic pressing [3] and pressureless sintering [4, 5]. The high fracture toughness was explained by a crack deflection model. It was calculated that an increase of the aspect ratio (length/diameter) of grains increased the contribution of crack deflection [6]. Similar microstructures have been developed during gas pressure sintering of α - Si_3N_4 powder [7–9]. The gas pressure sintering of α - Si_3N_4 powder resulted in “composite” microstructures with a small number of large rod-like grains and a large number of small equiaxial grains.

It has been reported that densification is accompanied by α to β phase transformation during hot-pressing [1, 10] and pressureless sintering [4, 5]. This information is sometimes referred to as if a higher α content is one of the important requirements for sinterable powders. It was shown, however, that β powders could be fully densified by hot-pressing [11] or pressureless sintering [12]. These facts suggest that phase transformation did not affect the sinterability of the powder, and rather give a large influence to grain growth. There are quite a few reports on quantitative evaluation of grain growth during sintering of α - Si_3N_4 powder [5, 13]. The abnormal grain growth of rod-like grains is related to the nucleation of large β grains at an intermediate stage of densification [5], but the effect of phase composition in the starting powder on the microstructure of sintered material is not well established.

The grain growth during gas pressure sintering of

β - Si_3N_4 powder has been studied in order to investigate the intrinsic nature of grain growth, where the problem of phase transformation could be eliminated [14]. A uniform microstructure developed during the sintering because of normal grain growth. The purpose of this investigation is to study the sintering behaviour of β - Si_3N_4 powder in 980 kPa N_2 at 1800–2000 °C and to compare it with that of α - Si_3N_4 . The results will be discussed in relation to the densification mechanism and resulting microstructures.

2. Experimental procedure

High-purity α - Si_3N_4 powder (TS-7 grade, Tohsoh Corp., Japan) was converted to β -powder by heating at 1900 °C in a high nitrogen pressure. The grain size was fairly large because of dendritic growth of β -crystals via the gas phase. It was then pulverized by jet-milling in a nitrogen atmosphere. The average particle size of processed β - Si_3N_4 corresponding to 50% cumulative weight in the size distribution curve was 1.7 μm . Although the particle size of β - Si_3N_4 was fairly large, further pulverization was not performed in order to avoid the oxidation of particle surfaces. The amount of metallic impurities was determined with inductively coupled plasma emission spectroscopy (ICP) after dissolving the powder in a Teflon capsule with a mixed solution of HF and HNO_3 . A Leco TC-336 was used to analyse oxygen in the powder. The results are listed in Table I. The amount of metallic impurities in processed β - Si_3N_4 was about the same as in the starting α - Si_3N_4 or as-fired β - Si_3N_4 powder. The amount of oxygen, on the other hand, was decreased by the heat treatment at 1900 °C and increased again by the pulverization.

The processed β - Si_3N_4 powder was mixed with 5 wt % Y_2O_3 and 2 wt % Al_2O_3 in n-hexane using a

TABLE I Characteristics of β - and α - Si_3N_4 powders.

Powder type	Metallic impurity (wt %)				Oxygen content (wt %)	Average particle size (μm)
	Al	Fe	Ca	Mg		
β (as-fired)	0.03	0.005	< 0.002	< 0.001	0.2	
β (processed)	0.03	0.007	0.003	0.001	1.3	1.7
α	0.01	0.004	< 0.002	< 0.001	1.0	0.6

Si_3N_4 ball mill. The dried powder was passed through a 60 mesh (0.25 mm) sieve to eliminate large agglomerates. About 3 g of the powder was pressed under 19.6 MPa in a die with 16 mm diameter. The disc was then cold-isostatically pressed under 196 MPa. The density of the compact was about 1.92 g cm^{-3} , which is a little higher than that from the finer α - Si_3N_4 powder of about 1.63 g cm^{-3} .

The compact was set in a BN crucible which was placed in a carbon susceptor. A carbon bar with a BN bar at one end was placed on the specimen and suspended from a dilatometer. The compact was covered with high-purity α - Si_3N_4 powder to minimize differences of shrinkage in the compact due to the temperature distribution. The sintering was performed by induction heating in 980 kPa (10 atm) N_2 at 1800–2000 °C. The heating rate was $30 \text{ }^\circ\text{C min}^{-1}$. Shrinkage was monitored by the dilatometer during heating.

The weight loss was measured after cooling. The bulk density was calculated from the specimen size and weight. The microstructure of sintered material was observed on fractured surfaces by a scanning electron microscope (SEM). The same experiments were carried out with α - Si_3N_4 to compare with β - Si_3N_4 .

3. Results and discussion

The density of sintered material after heating for 1 h is shown in Fig. 1. The materials fabricated from β - Si_3N_4 at 1800–1950 °C have a higher density than those made from α - Si_3N_4 . Although the initial density of the compact from β - Si_3N_4 powder was larger than

that from α - Si_3N_4 , the fact that the final density of material from β - Si_3N_4 at 1900 °C is larger than that from α - Si_3N_4 may indicate that β - Si_3N_4 powder has a higher sinterability than α - Si_3N_4 . This was also shown in pressureless sintering [12]. The difference in the density between β - and α - Si_3N_4 was very small at 1950 and 2000 °C, because the density of the materials approach the theoretical value of 3.25 g cm^{-3} . The weight loss after heating β - Si_3N_4 compact increased from 1.5% at 1800 °C to 2.9% at 2000 °C, which is about 1 and 2% lower, respectively, than that for α - Si_3N_4 . The weight loss is related to the decrease of silica content in the compact [15]. The weight loss results in a decrease in the amount and viscosity of the liquid phase. The present result showed that the silica layer on β - Si_3N_4 powder has a higher stability than that on α - Si_3N_4 powder because of the larger grain size. The higher sinterability of β - Si_3N_4 might be partly due to the higher silica content in the compacts.

The changes of shrinkage and shrinkage rate with temperature and heating time at 1850 and 1950 °C are plotted in Figs 2 and 3, respectively. It is known that the densification of Si_3N_4 with an oxide additive is due to the presence of a liquid phase, i.e. to liquid-phase sintering. The main processes for the sintering are rearrangement and solution–reprecipitation [16, 17]. The initial densification observed at 1400–1500 °C is by the rearrangement process [18]. The particles moved to pack closer by capillary forces. The shape and size of particles were the same as those of the starting powder. The next densification observed at $> 1600 \text{ }^\circ\text{C}$ was due to the solution–reprecipitation

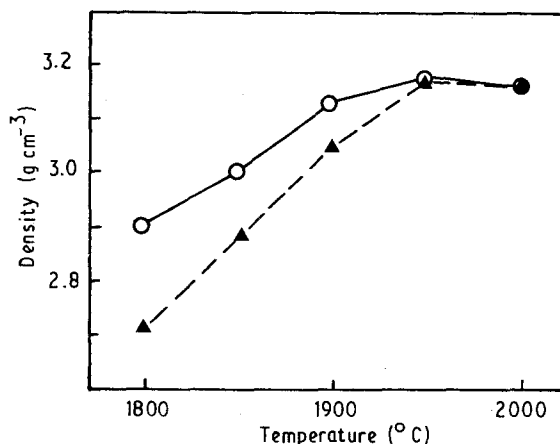


Figure 1 Bulk density of (\blacktriangle) α - Si_3N_4 and (\circ) β - Si_3N_4 after heating for 1 h in 980 kPa N_2 .

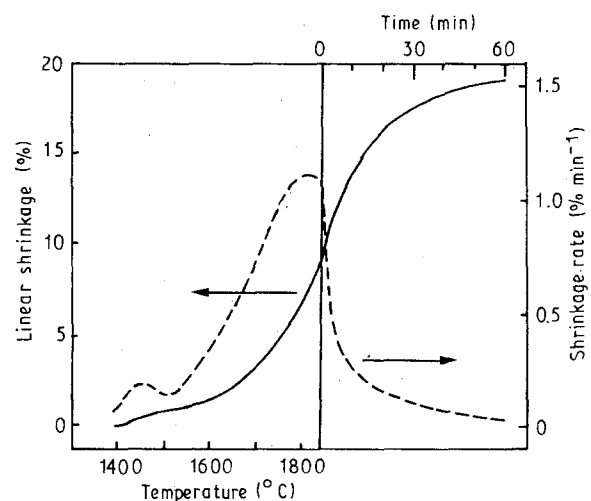


Figure 2 Linear shrinkage and shrinkage rate as a function of heating temperature, and of time at 1850 °C.

process. The process was accompanied by grain growth through the dissolution of small particles, diffusion of material in the liquid and reprecipitation on large particles. Thus the driving force for the densification and grain growth during sintering of

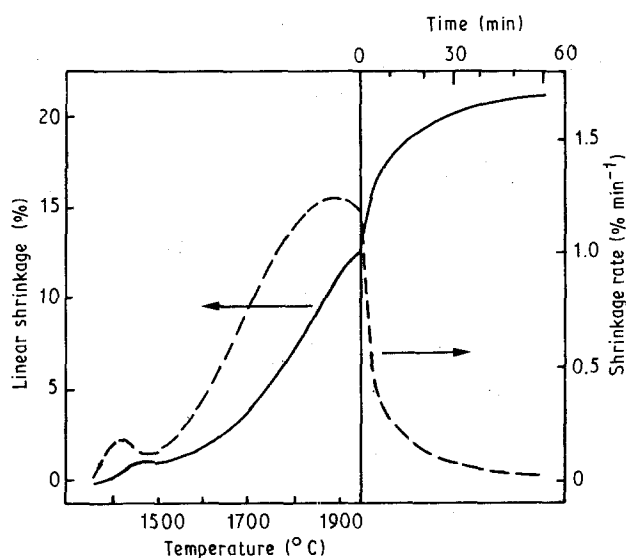


Figure 3 Linear shrinkage and shrinkage rate as a function of heating temperature, and of time at 1950°C.

β - Si_3N_4 is due only to size differences in the powder. The solution–reprecipitation process in the sintering of β - Si_3N_4 was in only one step at $> 1600^\circ\text{C}$, as shown in Figs 2 and 3.

The fractured surfaces of materials fabricated at 1850 and 1950°C for 1 h are shown in Fig. 4. The microstructures were fairly uniform compared to those from α - Si_3N_4 . This should be due to normal grain growth [14]. The final density of materials fabricated at 1850°C increased from 2.99 g cm^{-3} at 1 h to 3.21 g cm^{-3} at 4 h. Nevertheless, the microstructure after sintering for 4 h is about the same as that in material sintered for 1 h, as shown in Fig. 5. This is due to the low driving force for grain growth because of a uniform grain size distribution. Sintering for 8 h at 1850°C resulted in a decrease in the density to 3.19 g cm^{-3} .

A small expansion of the specimen was observed by the dilatometer at $> 4\text{ h}$. The occurrence of dewetting was revealed in a polished specimen (Fig. 6). This might be related to pore coalescence [17, 19]. The equilibrium pressure in a closed pore which is filled with a gas is expressed by [19, 20]

$$p_0 = p_{\text{ext}} + \frac{2\gamma_{lv}}{r_0} \quad (1)$$

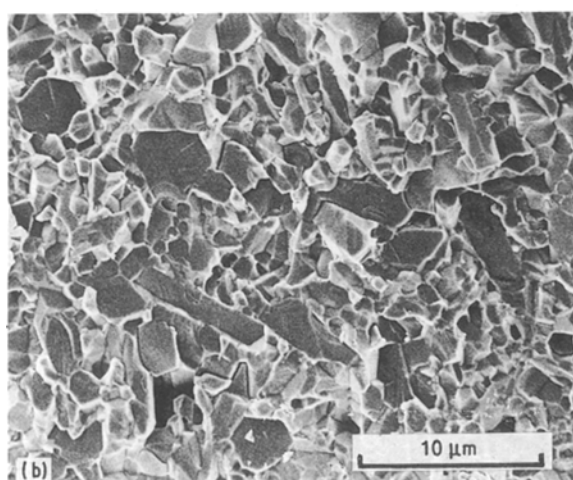
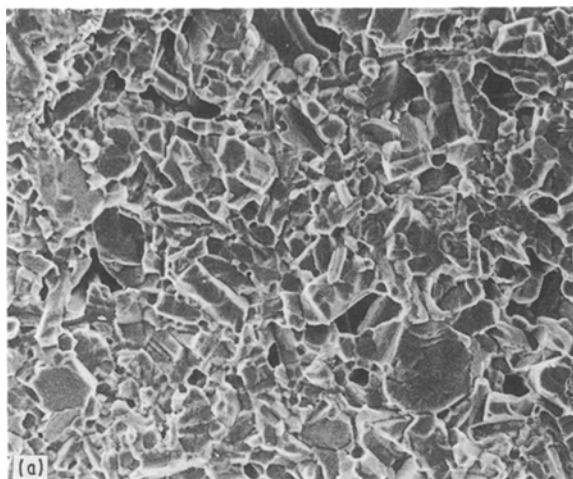


Figure 4 Fractured surface of material fabricated for 1 h at (a) 1850 and (b) 1950°C.

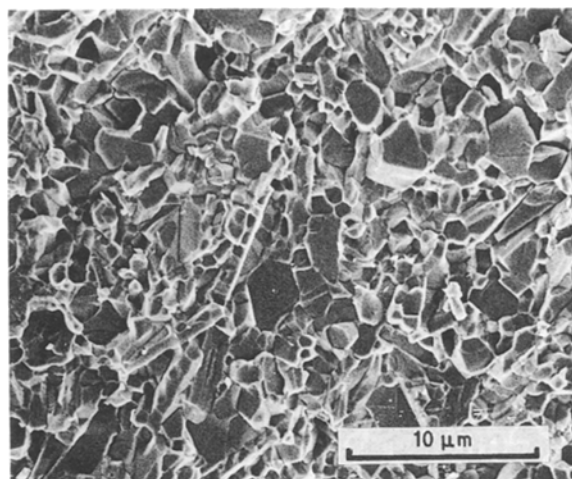


Figure 5 Fractured surface of material fabricated at 1850°C for 4 h.

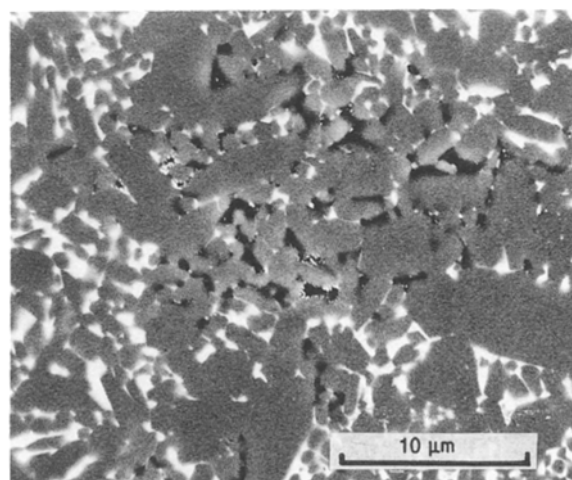


Figure 6 Dewetting of grains by pore coalescence.

where p_{ext} , γ_{lv} and r_0 are the external pressure over the specimen, liquid-vapour interfacial free energy and pore radius, respectively. If the radius of a pore grown by coalescence becomes r_1 where $r_1 > r_0$, the equilibrium pressure in the pore should become p_1 where $p_1 < p_0$. This means that the volume of the grown pore should become larger than the total volume of the pores which coalesced to reduce the internal pressure from p_0 to p_1 . This might be the reason that an expansion of the specimen was observed at the latter stage of heating at 1850°C.

In the gas pressure sintering of α -Si₃N₄, the solution-precipitation process was divided into two parts [7, 9]. In the first solution-precipitation process observed at 1550–1800°C, densification was followed by the α to β phase transformation. If the amount of additives was too small to fully densify by this process only, the phase transformation should complete at intermediate stage of densification. In the second solution-precipitation process observed at >1800°C, densification is accompanied by the dissolution of small β grains and reprecipitation on large β grains. The first densification process was, thus, also the nucleation process for grain growth. It must be noted that only a small number of β grains grew abnormally in the second densification process (Fig. 7). The large rod-like grains grew because of the wide range of the particle distribution [21].

There were many nuclei for grain growth in the sintering of β -Si₃N₄. This might be why only one densification process was observed at >1600°C. The rate of densification during heating to 1950°C and keeping for 1 h is plotted in Fig. 8 as a function of relative density. The simpler densification mechanism of β -Si₃N₄ compared to α -Si₃N₄ is revealed in the figure. The microstructure of sintered material is not sensitive to sintering temperature and time because of the single densification mechanism and uniform microstructure.

The kinetic equation for isothermal shrinkage is generally expressed by [16, 17],

$$\Delta L/L_0 = kr^{-4/3}t^{1/n} \quad (2)$$

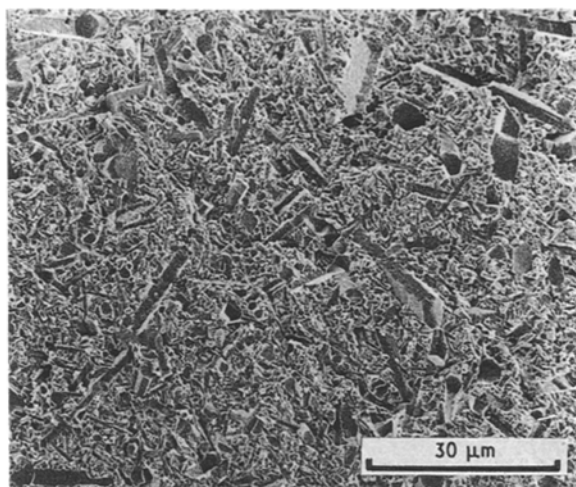


Figure 7 Fractured surface of material fabricated from α -Si₃N₄ at 1950°C for 1 h.

where k , r and t are constant, mean grain radius and sintering time, respectively. The value of n depends on the shape of grains and the densification mechanism. As the shape of the grains is basically a hexagonal prism [14], the equations for prismatic grains might be employed, i.e. $n = 5$ for diffusion-controlled and $n = 3$ for reaction-controlled mechanisms. The isothermal shrinkage obtained in the present work is plotted in Fig. 9. The calculated n value for sintering at 1800–1900°C was nearly 5, as predicted for diffusion-controlled sintering. The larger n value at 1950°C might be due to a lower densification rate because of coalescence of grains at the final stage of densification. Diffusion-controlled sintering was also reported for hot-pressing with MgO [13] and pressureless sintering with Y₂O₃ [22]. The same kinetics has been reported for the grain growth of silicon nitride [13].

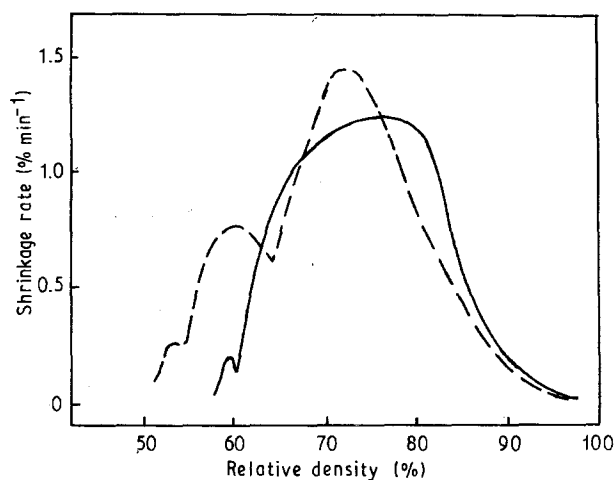


Figure 8 Plot of shrinkage rate during heating to 1950°C and keeping there for 1 h, as a function of relative density: (—) α -Si₃N₄, (—) β -Si₃N₄.

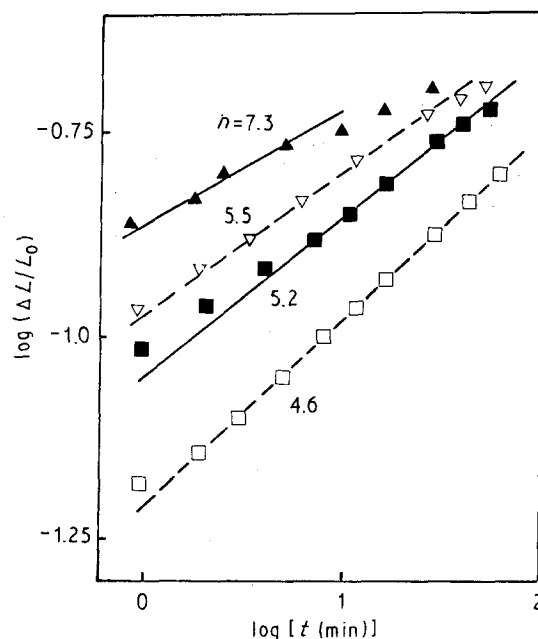


Figure 9 Plot of $\log(\Delta L/L_0)$ as a function of $\log t$ got sintering at (□) 1800, (■) 1850, (▽) 1900 and (▲) 1950°C for 1 h.

4. Summary

It was shown that β - Si_3N_4 powder had a higher sinterability than that of α - Si_3N_4 in gas pressure sintering in 980 kPa N_2 at 1800–2000 °C. Diffusion at the grain-boundary liquid phase was believed to be the rate-determining step. The densification curves for β - Si_3N_4 revealed that the kinetics of densification was simpler than that for α - Si_3N_4 . The microstructures of materials from β - Si_3N_4 were more uniform than those from α - Si_3N_4 because of the absence of phase transformation during sintering. The pore coalescence observed after prolonged heating resulted in a dewetting of grains and a density decrease.

References

1. G. HIMSLT, H. KNOCH, H. HUEBNER and F. W. KLEINLEIN, *J. Amer. Ceram. Soc.* **62** (1979) 29.
2. F. F. LANGE, *ibid.* **62** (1979) 428.
3. J. HEINRICH and M. BOEHMER, *ibid.* **67** (1984) C-75.
4. K. MATSUHIRO and T. TAKAHASHI, in Proceedings of MRS International Meeting on Advanced Materials, Vol. 5, edited by Y. Hamano, O. Kamigaito, T. Kishi and M. Sakai (Materials Research Society, Pittsburg, PA, USA, 1989) p. 11.
5. G. WOETTING, B. KANKA and G. ZIEGLER, in "Non-oxide Technical and Engineering Ceramics", edited by S. Hampshire (Elsevier Applied Science, Essex, UK, 1986) p. 83.
6. K. T. FABER and A. G. EVANS, *Acta Metall.* **31** (1983) 577.
7. M. MITOMO and K. MIZUNO, *Yogyo-Kyokai-Shi* **94** (1986) 106.
8. E. TANI, S. UMEBAYASHI, K. KISHI, K. KOBAYASHI and N. NISHIJIMA, *Amer. Ceram. Soc. Bull.* **65** (1986) 1311.
9. M. MITOMO, N. YANG, Y. KISHI and Y. BANDO, *J. Mater. Sci.* **23** (1988) 3413.
10. L. J. BOWEN, R. J. WESTON, T. G. CARRUTHERS and R. J. BROOK, *ibid.* **13** (1978) 341.
11. G. R. TERWILLIGER and F. F. LANGE, *J. Amer. Ceram. Soc.* **57** (1974) 25.
12. D.-D. LEE, S.-J. L. KANG, G. PETZOW and D. N. YOON, *ibid.* **73** (1990) 767.
13. C. M. HWANG, T. Y. TIEN and I-WEI CHEN, in "Sintering '87", edited by S. Somiya, M. Shimada, M. Yoshimura and R. Watanabe (Elsevier Science Publications, NY, USA, 1988) p. 1034.
14. M. MITOMO, M. TSUTSUMI, H. TANAKA, S. UENOSONO and F. SAITO, *J. Amer. Ceram. Soc.* **73** (1990) 2441.
15. N. HIROSAKI and A. OKADA, *ibid.* **72** (1989) 2359.
16. W. D. KINGERY, *J. Appl. Phys.* **30** (1959) 301.
17. R. M. GERMAN, in "Liquid Phase Sintering" (Plenum, NY, USA, 1985) p. 127.
18. M. MITOMO, *J. Mater. Sci.* **11** (1976) 1103.
19. C. GRESKOVICH, *J. Amer. Ceram. Soc.* **64** (1981) 725.
20. S.-J. L. KANG, P. GREIL, M. MITOMO and J. H. MOON, *ibid.* **72** (1989) 1166.
21. M. MITOMO, S. UENOSONO and F. SAITO, unpublished work.
22. K. H. JACK, in Final Technical Report DAERO-78-G-012 (London, 1978) p. 3.

Received 14 June
and accepted 26 June 1990